INTERFACE '96

This paper was published in the proceedings of the
Olin Microlithography Seminar, Interface '96, pp. 325-336.
It is made available as an electronic reprint with permission of
Olin Microelectronic Materials, Inc.

Reducing Proximity Effects in Optical Lithography

Chris A. Mack
FINLE Technologies, Inc.
P.O. Box 162712, Austin, Texas 78716 USA

Abstract

Using simulation, the influence of stepper parameters on optical proximity effects is explored. In particular, numerical aperture and partial coherence will be examined for a variety of feature sizes and types. Both one-dimensional and two-dimensional mask features will be studied. The impact of resist contrast will also be explored. In addition to the iso-dense print bias as a metric of proximity effects, the depth of focus as an *overlapping* of two focus-exposure process windows, one for the isolated line and one for the dense line, will be used. The optimum NA and σ will give the maximum depth of focus calculated from the overlapped process window. Finally, the statistical CD distribution methodology will be used to find the stepper settings that minimize the linewidth distribution spread for a given process.

I. Introduction

Proximity effects are the variations in the linewidth of a feature (or the shape for a 2-D pattern) as a function of the proximity of other nearby features. The concept of proximity effects became prominent many years ago when it was observed that electron beam lithography can exhibit extreme proximity effects (backscattered electrons can travel many microns, exposing photoresist at nearby features). Optical proximity effects refer to those proximity effects that occur during optical lithography (even though they may not be caused by optical phenomenon!). The simplest example of an optical proximity effect is the difference in printed linewidth between an isolated line and a line in a dense array of equal lines and spaces, called the *iso-dense print bias*.

Although many factors may affect the iso-dense print bias, such as developer flow, PEB diffusion or proximity dependent surface inhibition effects, in general this bias is the result of optics -- the aerial images for dense and isolated lines are different. For high resolution features, the diffraction patterns from isolated and dense lines are significantly different. The result is different aerial images, as shown in Figure 1. In this case, the isolated line will print wider than the dense line (assuming a positive photoresist), giving a positive iso-dense print bias. It is important to note that this result is not a "failing" of the optical system, but a natural consequence of the physics of imaging. Also, aberrations in the optical system can change the magnitude of the bias, sometimes significantly.

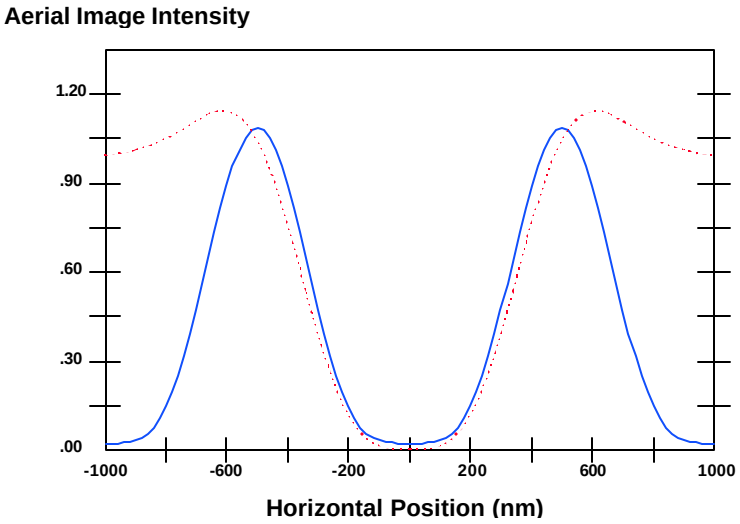

Figure 1. In general, the optical proximity effect is caused by optics. Here the aerial image of an isolated 0.5 μm line (dashed) is wider than the image of a dense line (solid).

To further explore the proximity effect of lines and spaces, consider the width of a 0.5 μm line as a function of pitch (i.e., as a function of the proximity of another 0.5 μm line), as shown in Figure 2. Notice that a pitch of 1.4 times the equal line-space pitch produces, in this case, the largest proximity effect. A simple way of characterizing this optical proximity effect is to express the difference in printed linewidth between an isolated line and a line in a dense array of equal lines and spaces (the iso-dense print bias). Although the iso-dense print bias is generally not the largest proximity effect possible for lines and spaces, the convenience of this parameter makes it a logical choice for monitoring proximity effects in general.

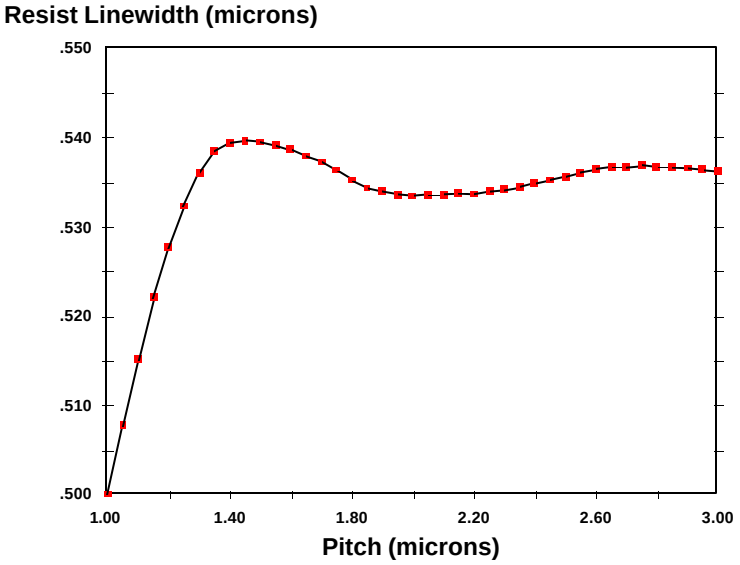

Figure 2. Variation of a feature linewidth as a function of the nearest neighbor distance (pitch) reveals that the maximum proximity effect is often not the iso-dense print bias (i-line, NA = 0.52, σ = 0.5).

The proximity effect is very feature size dependent. For large features, the diffraction patterns for isolated and dense lines are similar, giving very little differences in the aerial images. As feature size shrinks, the differences grow. Figure 3 gives an example of how the iso-dense print bias increases dramatically as the feature size approaches the resolution limit of the exposure tool (in this case, with a partial coherence of $\sigma = 0.5$). The iso-dense bias is quite small for feature sizes above $k_1 = wNA/\lambda = 1.0$, and increases as k_1 goes down to 0.6. Notice that the iso-dense bias begins to decrease at the smallest features. As we shall see later, the iso-dense print bias will begin a rapid fall as the resolution limit is approached.

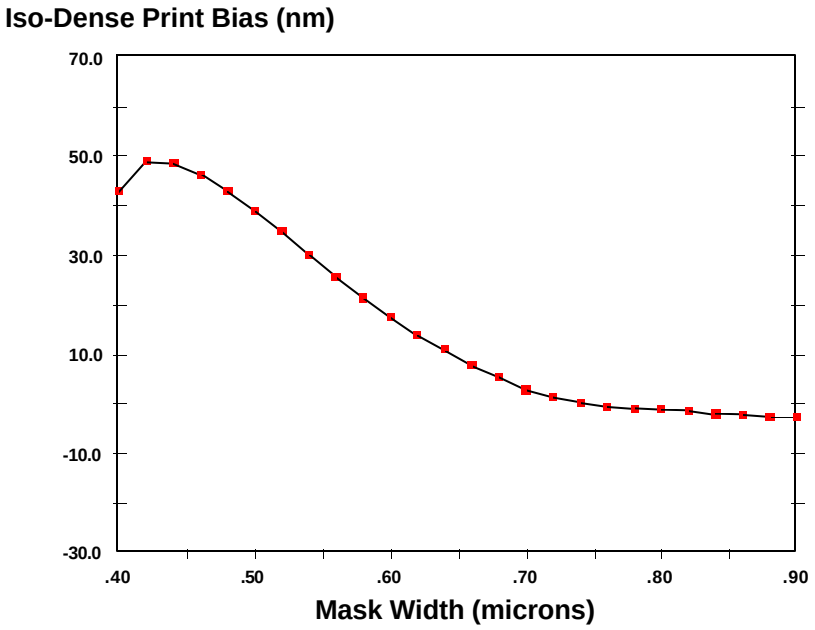

Figure 3. Feature sizes below 0.7μm ($k_1 = wNA/\lambda = 1.0$) show increasing proximity effects (λ = 365nm, NA = 0.52, $\sigma = 0.5$), until it reaches a peak at 0.42μm ($k_1 = 0.6$).

II. Effect of Optical Parameters

Since the iso-dense print bias is predominantly an optical effect, one would expect that the optical parameters of the stepper would affect the magnitude of the bias. It is well known that the illumination partial coherence greatly influences proximity effects. Figure 4 emphasizes this point by showing fairly dramatic differences in the iso-dense print bias among the different partial coherence values. A partial coherence of 0.5 gives the best results for larger features ($k_1 \geq 1$), $\sigma = 0.7$ shows less feature size dependence, while smaller partial coherences show more feature size dependence. One can see that for any feature size there will be at least one value of the partial coherence which drives the iso-dense print bias to zero. Unfortunately, zero bias at one feature size does not give zero bias at other

sizes. Also note that the feature size at which the iso-dense print bias reaches a maximum decreases with decreasing partial coherence.

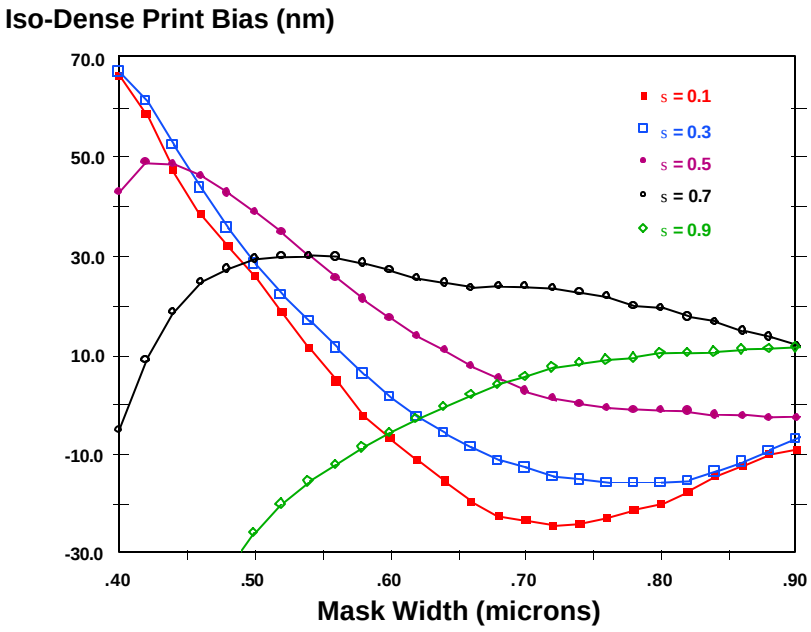

Figure 4. Partial coherence significantly affects the iso-dense print bias (λ = 365nm, NA = 0.52).

Modern steppers allow the variation of both numerical aperture (*NA*) and partial coherence over certain ranges. Although these optical parameters could be used to maximize the depth of focus, they can also be used to minimize the iso-dense print bias. Figure 5 shows a contour plot of iso-dense print bias as both NA and σ are varied for 0.5 μm (k_1 = 0.71) and 0.7 μm (k_1 = 1.0) feature sizes. The shaded areas show the ranges of NA and σ that keep the bias within ±10 nm (an arbitrary specification). The larger feature has a wide range of numerical apertures and partial coherences which produce a small iso-dense bias. Note that for this feature a partial coherence of 0.9 provides small bias over the full range of numerical aperture, but a partial coherence of 0.8 produces a larger bias over the full range of numerical aperture. Small σ at high numerical apertures also give small iso-dense print bias. The rule of thumb that larger σ means less proximity effects is quite inaccurate. The smaller 0.5 μm feature has a much smaller "window" of acceptable stepper settings. Typical partial coherence values of 0.5 - 0.7 in particular provide poor performance. Either higher or lower σ is needed, as well as a high numerical aperture. Note that there is some overlap between the two feature sizes. It is possible to find a single stepper setting that will produce small iso-dense print bias for both of these features.

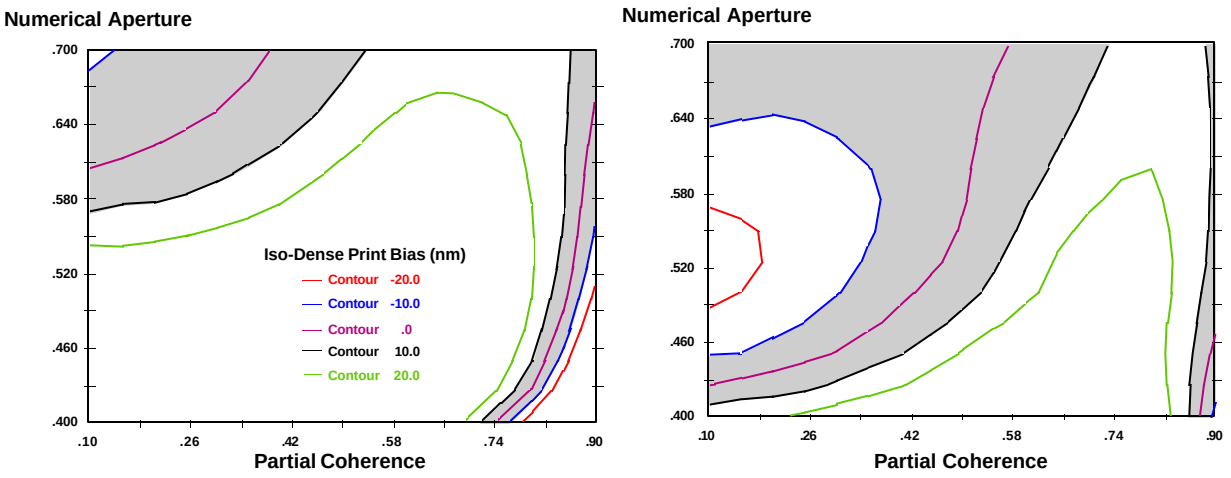

(a) (b)

Figure 5. Contours of constant iso-dense print bias for (a) 0.5 μm and (b) 0.7 μm lines. The shaded areas show regions where the print bias is less than ±10nm.

III. Effect of Resist Contrast

All of the results shown above were generated using simulation assuming a typical i-line photoresist. How significant is the photoresist in determining the iso-dense print bias? Do resist properties (especially the resist contrast) impact the optimization of numerical aperture and partial coherence in reducing proximity effects? If a mask is biased to reduce proximity effects, will the mask work only with one resist? Arthur and Martin [1] have shown, using simulations, that the resist does play a role in determining the magnitude of the iso-dense print bias. By systematically studying most of the parameters used to simulate resist exposure and development, they found that only the resist dissolution selectivity parameter *n* of the Mack dissolution model [2] had a significant impact on proximity effects. The dissolution selectivity parameter is directly proportional to resist contrast [3], thus confirming the expected result that different resist contrast produces different iso-dense print bias.

To investigate more thoroughly the impact of the resist on the iso-dense print bias, this bias was simulated for different feature sizes, different partial coherences, and different dissolution selectivity parameters. Figure 6 shows the results. Each plot shows, for a given partial coherence, the iso-dense print bias as a function of mask size for different resist *n* parameters. The dissolution selectivity parameter *n* was varied from a moderate-to-low value of 4, a typical value of 5.5, a moderate-to-high value of 7, a high resist contrast with an *n* value of 10, and finally, a super-high dissolution selectivity of 16, corresponding to an advanced resist of the future.

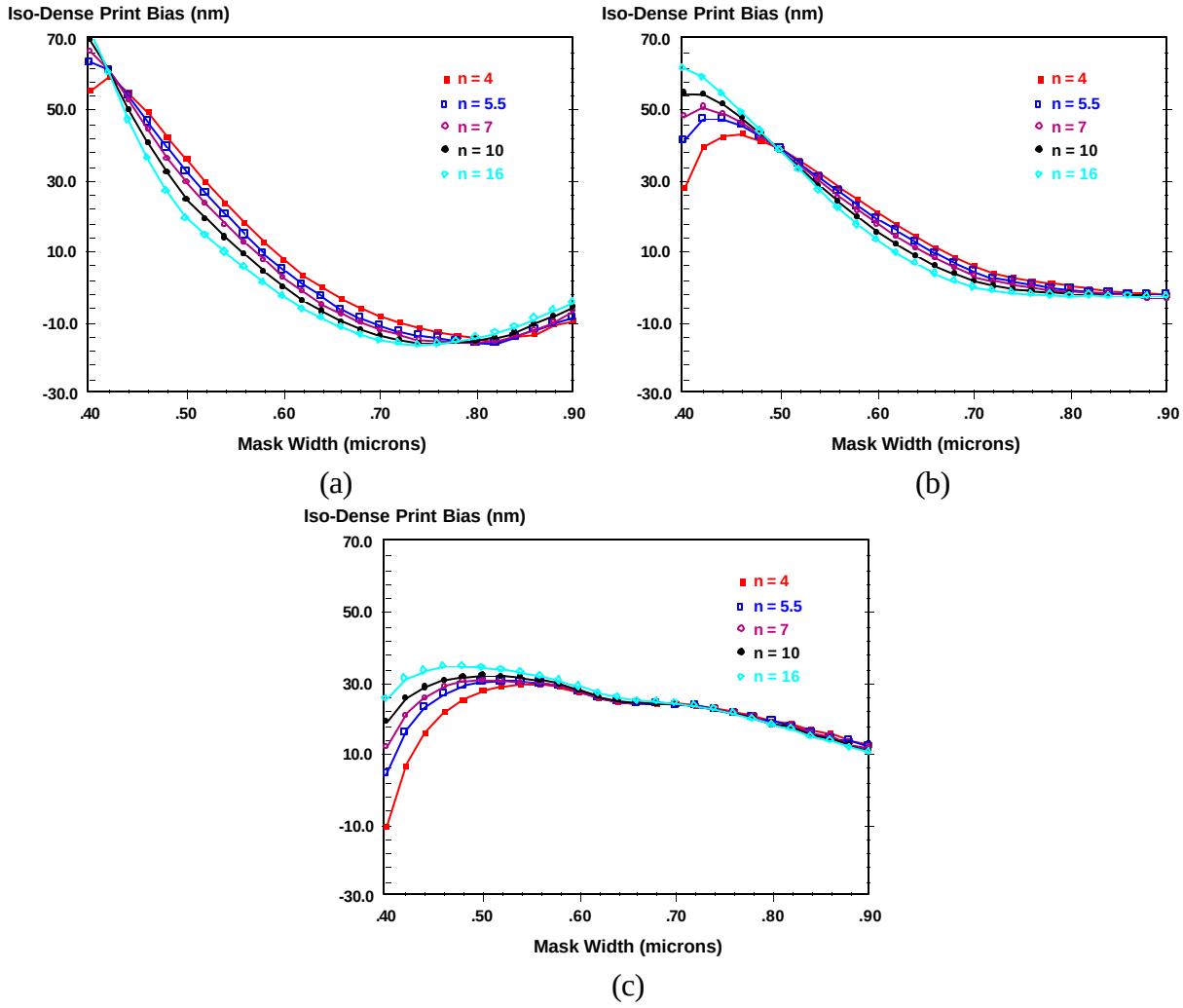

Figure 6. Impact of resist contrast (which is proportional to the resist dissolution selectivity parameter n) on the iso-dense print bias. This print bias is shown as a function of mask feature size for partial coherences of (a) $\sigma = 0.3$, (b) $\sigma = 0.5$, and (c) $\sigma = 0.7$ (i-line, NA = 0.52).

Some interesting trends can be observed from the results of Figure 6. In all cases, resist contrast (via the dissolution selectivity parameter n) has very little effect on iso-dense print bias for larger features. For the $\sigma = 0.7$ case, mask widths above 0.55 μm ($k_1 = 0.78$) showed very little variation of the iso-dense print bias with resist contrast. Smaller features, however, began to exhibit more variation. At 0.4 μm features, the iso-dense print bias varied from -10 nm to +25 nm depending on the resist *n* parameter. For $\sigma = 0.5$, features below 0.50 μm ($k_1 = 0.71$) began showing increased sensitivity to resist contrast. For $\sigma = 0.3$, the transition occurred at a feature size of 0.42 μm ($k_1 = 0.60$). However, for this partial coherence, there was considerable variation in the iso-dense print bias with resist *n* parameter at larger features as well (up to 16 nm).

Focusing on the $\sigma = 0.5$ case, several interesting trends can be observed. Smaller features show larger iso-dense print bias up to a point, after which the iso-dense print bias decreases. This decrease is due, essentially, to the resolution limitation of the process. As the dense lines become

harder to resolve, their widths grow reducing the iso-dense print bias. At this point, the dense lines are quite susceptible to scumming even though the isolated lines are easily resolved (equivalent to a large negative iso-dense print bias). Thus, at the "resolution limit", the iso-dense print bias reverses its natural trend. Higher contrast resist will push the resolution limit to a lower feature size. Thus, as seen in Figure 6b, the point at which the iso-dense print bias reaches its maximum occurs at a lower feature size as well. At $\sigma = 0.5$, the 0.4 μm features show a 34 nm range in the iso-dense print bias as a function of resist contrast.

IV. Finding the Optimum Stepper

A judicious choice of numerical aperture and partial coherence is needed to obtain the best depth of focus. What if the optimum settings for good depth of focus do not coincide with the optimum settings for small iso-dense print bias? As is often the case, good focus performance may be required for both dense and isolated lines at the same time. In this case, one approach is to evaluate the depth of focus as an *overlapping* of two focus-exposure process windows, one for the isolated line and one for the dense line. The optimum NA and σ will give the maximum depth of focus calculated from the overlapped process window.

For example, Figure 5a shows a large number of NA and σ configurations which give zero iso-dense print bias (at nominal exposure and best focus) for 0.5μm features. Thus, the settings of NA = 0.65, $\sigma = 0.3$ could be used as well as NA = 0.44, $\sigma = 0.8$. But how do these settings affect other aspects of the lithographic process, in particular the focus-exposure response? Figure 7 examines this response by showing, at each of these two stepper settings, the overlap of the focus-exposure process window for dense and isolated lines. (The process window is the region of focus and exposure that keeps the linewidth within specification, in this case ±10% of the nominal.)

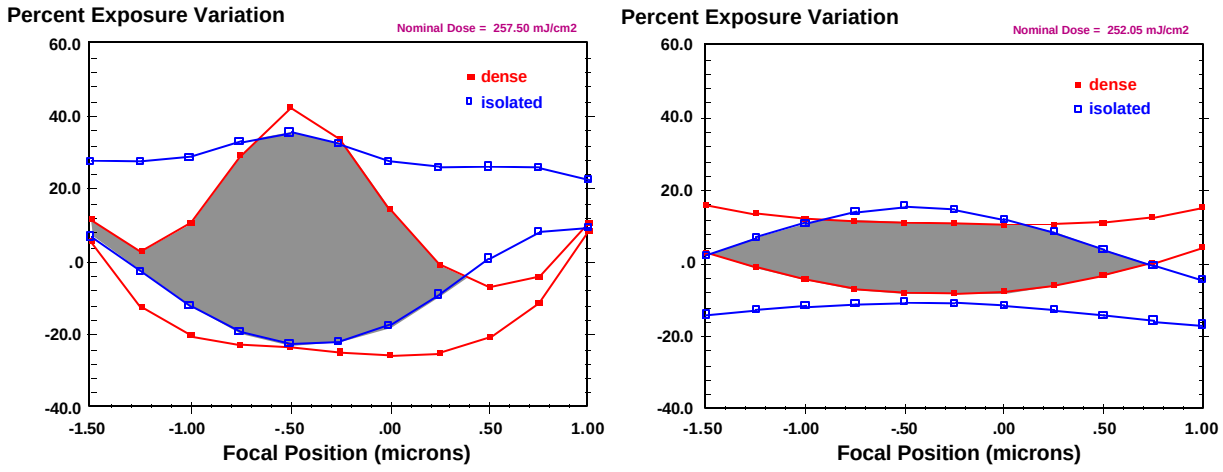

Figure 7. Overlapping process windows for dense and isolated 0.5μm lines for (a) NA = 0.65, $\sigma = 0.3$ and (b) NA = 0.44, $\sigma = 0.8$. Gray area indicates the overlap region, the region of focus and exposure that keeps both dense and isolated lines within ±10% of the nominal.

In both Figure 7a and Figure 7b, the centers of the dense and isolated process windows fall at the same value of focus and exposure. Thus, at this value (best focus and nominal exposure) there is no iso-dense print bias for either of the stepper settings. However, the size and shape of the overlapping regions for these two cases is quite different. The low NA case (Figure 7b) shows a much smaller overlapped process window than the high NA case (Figure 7a). One could imagine, by examining Figure 7, that the maximum overlap of the dense and isolated processes windows may not necessarily occur at stepper settings that give zero iso-dense print bias at nominal focus and exposure. Thus, a more appropriate way of optimizing NA and σ would be to find the settings which give the maximum overlap of the focus exposure process windows.

Ultimately, the best approach for finding the optimum NA and σ is to use a metric of lithographic performance which reflects manufacturing realities. All lithography processes exhibit errors in the process, some systematic and some random, which result in errors in the final printed linewidth. The result is a distribution of CD values (across the chip, across the wafer, wafer to wafer). Proximity effects, for example, will cause a spread of the final CD distribution, as will errors in focus and exposure. The goal of process optimization is to reduce the spread of the CD distribution.

Several authors have investigated the use of lithography simulation to predict CD distributions [5-9]. First, the simulator is used to predict the *response* of a process to an error (such as linewidth versus exposure). Then this response is sampled by a known error (such as an error distribution of exposure with a mean and standard deviation) to produce a distribution of CDs (Figure 8). Of course, more than one input variable can be used.

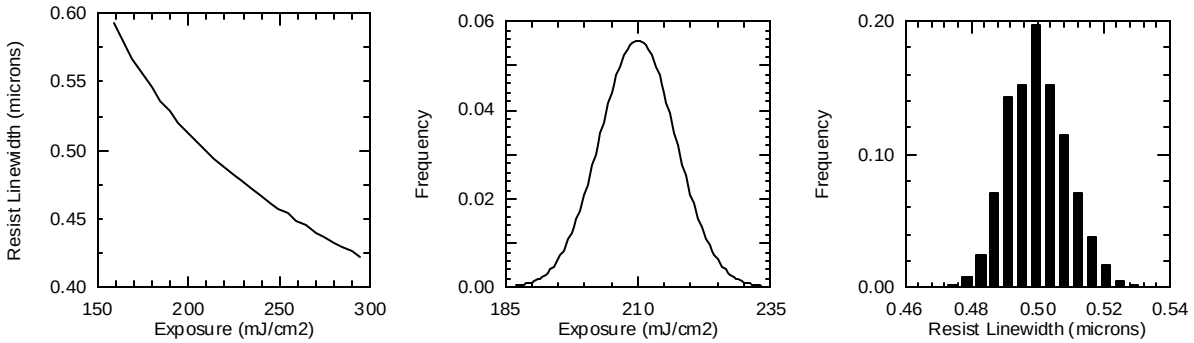

Figure 8. Process flow for calculation of the final CD distribution (a one-dimensional example).

The CD distribution approach can be used to find the optimum NA and σ of a stepper. For a known range of exposure and focus errors, the optimum NA and σ values would be those that gave the minimum spread of the CD distribution (more correctly, the maximum percentage of CDs which fall within the linewidth specifications, called the CD yield). If the input process response includes both dense and isolated lines, then the analysis would include proximity effects as well. Figure 9 shows such an analysis. PROLITH/2 [10] was used to predict linewidth as a function of NA, σ, focus, exposure

and pitch (dense and isolated) resulting in the calculation of 500,000 linewidths. The resulting process response space was analyzed with the ProCD [10] statistical analysis package. Focus and exposure errors were assumed to be normally distributed with standard deviations of 0.3μm and 15 mJ/cm^2, respectively. The means of each distribution were always adjusted to maximize the CD yield (resulting in the most logical definition of best focus and exposure). An equal number of dense and isolated lines were used in each distribution.

As an example of the use of the calculated CD distribution technique, we can compare the two steppers described above: NA = 0.65 and σ = 0.3 versus NA = 0.44 and σ = 0.8. Both showed zero iso-dense print bias for 0.5 μm lines at nominal focus and exposure. The overlapping process windows, however, indicated a difference in focus-exposure response. The CD distributions shown in Figure 9 clearly illustrate that the higher NA system is better in this case. Figure 9a shows the resulting CD distribution for the NA = 0.65 system with a CD yield of 98.5%. The NA = 0.44 system, shown in Figure 9b, produced a CD yield of only 89.2% for the same focus and exposure errors.

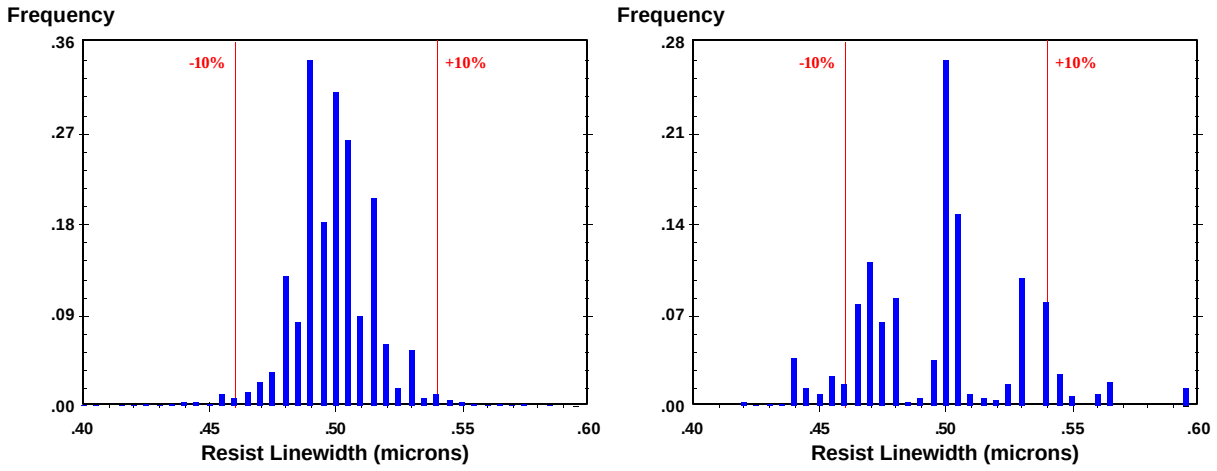

Figure 9. Calculated CD distributions of 0.5μm lines for (a) NA = 0.65, σ = 0.3 and (b) NA = 0.44, σ = 0.8. Distributions are for equal numbers of dense and isolated lines with normal focus and exposure errors with standard deviations of 0.3μm and 15 mJ/cm^2, respectively. The mean values of the focus and exposure errors were adjusted to give the maximum CD yield.

V. Two-Dimensional Proximity Effects

One-dimensional features such as lines and spaces are not only important in semiconductor devices but they provide the simplest features for evaluating lithographic principles such as proximity effects. There are, however, many two-dimensional proximity effects which cannot be explored by examining only simple 1-D patterns. One very important 2-D proximity effect is line-end shortening. A minimum dimension line will be rounded at the end so that the position of the end is considerably shortened relative to the position of the end of the line on the mask. The most common "fix" for this problem is to draw the line on the mask longer than the desired line on the wafer. This approach runs

into problems when the end of the line is in close proximity to another feature. Figure 10 shows an example of one such case.

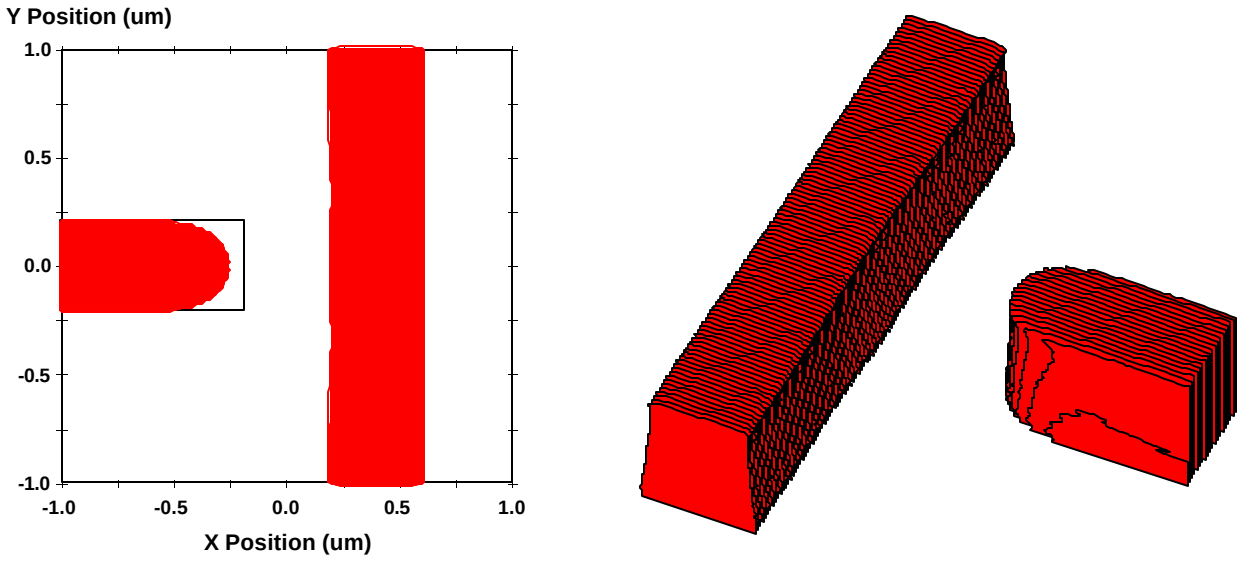

Figure 10. Line-end shortening is an important two-dimensional proximity effect (top-down and side-angle views shown here).

The same methodology applied above to 1-D patterns can be applied to 2-D patterns as well. Thus, line-end shortening as a function of focus and exposure can be determined and used as a more realistic metric of the proximity effect, as seen in Figure 11. NA and σ will also impact these results. For more complicated 2-D patterns, the Critical Shape Error [11] can be used to optimize the printing of these features.

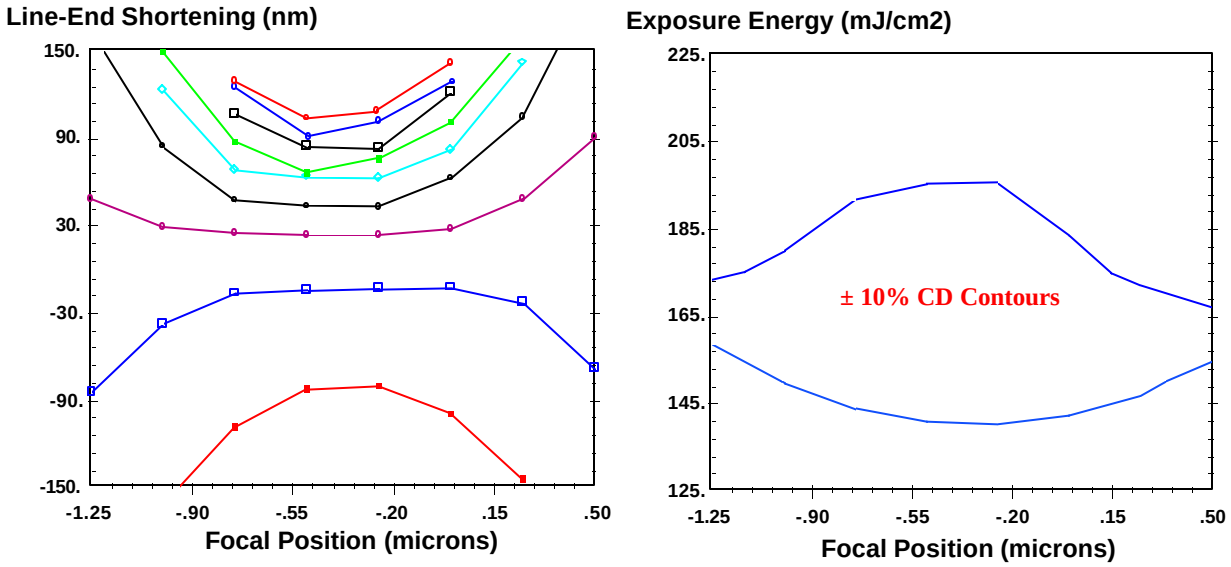

Figure 11. Focus-Exposure response of the line-end shortening example of Figure 10: a) Bossung curves and b) process window made from contours of ±10% line-end deviation.

VI. Conclusions

Proximity effects will play an increasingly important role in optical lithography as features sizes are pushed to the resolution limits. As this work has shown, the optical parameters of the stepper or scanner have a significant impact on the magnitude of the proximity effects. Projection systems with variable NA and σ offer a unique opportunity to minimize these optical proximity effects, at least for specific feature sizes. However, looking at the proximity effects just at nominal exposure and focus can be quite misleading. Process window overlap for dense and isolated lines gives a better indication of real-world performance. The ultimate approach, however, is the use of the calculated CD distribution. This method provides a convenient and easily understandable tool for optimizing the numerical aperture and partial coherence of a stepper/scanner which reflects manufacturing realities.

References

1. Graham Arthur and Brian Martin, "Investigation of Photoresist-Specific Optical Proximity Effect," *Micro- and Nano-Engineering '95*, Aix-en-Provence, France (Sep. 1995).

2. C. A. Mack, "Development of Positive Photoresist," *Jour. Electrochemical Society*, Vol. 134, No. 1 (Jan. 1987) pp. 148-152.

3. C. A. Mack, "Lithographic Optimization Using Photoresist Contrast," *KTI Microlithography Seminar, Proc.*, (1990) pp. 1-12, and *Microelectronics Manufacturing Technology*, Vol. 14, No. 1 (Jan. 1991) pp. 36-42.

4. Graham Arthur and Brian Martin, "Minimising Optical Proximity Effect at Sub-Half-Micron Resolution by the Variation of Stepper Lens Operating Conditions at i-line, 248nm and 193nm Wavelengths," *Metrology, Inspection, and Process Control for Microlithography X, Proc.*, SPIE Vol. 2725 (1996).

5. C. A. Mack and E. W. Charrier, "Yield Modeling for Photolithography," *OCG Microlithography Seminar, Proc.*, (1994) pp. 171-182.

6. E. W. Charrier and C. A. Mack, "Yield Modeling and Enhancement for Optical Lithography," *Optical/Laser Microlithography VIII, Proc.*, SPIE Vol. 2440 (1995) pp. 435-447.

7. E. W. Charrier, C. J. Progler and C. A. Mack, "Comparison of Simulated and Experimental CD-Limited Yield for a Submicron I-Line Processes," *Microelectronic Manufacturing Yield, Reliability, and Failure Analysis, Proc.*, SPIE Vol. 2635 (1995) pp. 84-94, and *Solid State Technology*, Vol. 38, No. 11 (Nov. 1995) pp. 105-112.

8. K. Ronse, R. Pforr, M. Op de Beeck, L. Van den hove, "CD Control: The Limiting Factor for I-Line and Deep-UV Lithography," *OCG Microlithography Seminar, Proc.*, (1995) pp. 241-254.

9. Z. Krivokapic, W. D. Heavlin, D. Kyser, "Process Capabilities of Critical Dimensions at Gate Mask," *Optical/Laser Microlithography VIII, Proc.*, SPIE Vol. 2440 (1995) pp. 480-491.

10. FINLE Technologies, Inc., Austin, Texas

11. C. A. Mack, "Evaluation of Proximity Effects Using Three-Dimensional Optical Lithography Simulation," *Optical/Laser Microlithography VIII, Proc.*, SPIE Vol. 2726 (1996).